

# Explanation of positive and negative PICTS peaks in SI-GaAs

S. Schmerler · T. Hahn · S. Hahn · J. R. Niklas ·  
B. Gründig-Wendrock

Received: 8 November 2007 / Accepted: 28 December 2007  
© Springer Science+Business Media, LLC 2008

**Abstract** A system of rate equations was used to study the unusual behavior of the EL2 defect in SI-GaAs. Experimental results show a strong correlation between the position of the Fermi level and the appearance of either negative or positive EL2 peaks. The applied model reproduces experimental results and provides a mechanism which explains the occurrence of negative EL2 peaks. Besides the numerical simulation we also adapted a simplified trap model which leads to a qualitative understanding of the negative PICTS peak effect. Furthermore, the existence of negative peaks can be viewed as evidence for the presence of a recombination center besides the EL2 in the analyzed samples.

## 1 Introduction

Microwave detected photo induced current transient spectroscopy (MD-PICTS) is a well-known tool for the contact-less and non-destructive investigation of electrical properties of defects in semiconductors [1–3]. Especially in semi-insulating GaAs (SI-GaAs) positive and negative PICTS peaks, which are mostly attributed to the EL2 defect, can be observed at temperatures above  $\approx 350$  K,

whereas the exact peak maximum temperature depends on the details of the applied PICTS data evaluation. The origin of this negative PICTS signal was addressed several times, but so far not clarified completely [4–8]. Essentially, most explanations involve a single deep level (usually the EL2), which interacts with both bands.

Here we present a model which is able to explain the measured dependence of the EL2 PICTS peak sign on the acceptor concentration (i.e. the Fermi level in the samples). The model assumes an additional recombination center (RC), which has been suggested several times [9–11]. It will be shown that such a center is an important precondition for the formation of negative EL2 peaks.

## 2 The rate equation system

According to Fig. 1, the rate equations take the form of Eq. 1.

$$\dot{n} = G_{\text{th}} + G_{\text{opt}} - R_{\text{bb}} - R_{\text{Aug}} + C - D \quad (1a)$$

$$\dot{p} = G_{\text{th}} + G_{\text{opt}} - R_{\text{bb}} - R_{\text{Aug}} + E - F \quad (1b)$$

$$\dot{n}_{\text{T}} = E - F - C + D \quad (1c)$$

Individual rates have the usual form.

$$G_{\text{th}} = [N_{\text{V}} - p] \sigma_{\text{bb}} v_{\text{n}} \times \exp(-[E_{\text{C}} - E_{\text{V}}]/kT) [N_{\text{C}} - n] \quad (2a)$$

$$R_{\text{bb}} = n \sigma_{\text{bb}} v_{\text{n}} p \quad (2b)$$

$$C = n_{\text{T}} \sigma_{\text{n}} v_{\text{n}} \times \exp(-[E_{\text{C}} - E_{\text{T}}]/kT) [N_{\text{C}} - n] \quad (2c)$$

$$D = n \sigma_{\text{n}} v_{\text{n}} [N_{\text{T}} - n_{\text{T}}] \quad (2d)$$

S. Schmerler (✉) · T. Hahn · S. Hahn · J. R. Niklas  
Institute for Experimental Physics, TU Bergakademie Freiberg,  
Leipziger Str. 23, 09599 Freiberg, Germany  
e-mail: s.schmerler@gmx.net

B. Gründig-Wendrock  
Deutsche Solar AG, Berthelsdorfer Str. 11A,  
09599 Freiberg, Germany

$$E = [N_V - p] \sigma_p v_p \times \exp(-[E_T - E_V]/kT) [N_T - n_T] \tag{2e}$$

$$F = n_T \sigma_p v_p p \tag{2f}$$

$$R_{aug} = (C_n n + C_p p) (np - n_i^2) \tag{2g}$$

Here  $N_V$  and  $N_C$  are the effective densities of states for the VB and CB,  $v_n$  and  $v_p$  the average thermal carrier velocities,  $\sigma_n$  and  $\sigma_p$  the cross sections of the defect level for CB and VB interaction,  $\sigma_{bb}$  the radiative band-band recombination cross section [12],  $C_n$  and  $C_p$  the Auger coefficients and  $n_i$  the intrinsic carrier concentration. We take into account optical ( $G_{opt}$ ) and thermal ( $G_{th}$ ) band-band generation as well as direct band-band recombination ( $R_{bb}$ ) and Auger recombination ( $R_{aug}$ ). However, thermal band-band generation and recombination play a minor role when defects with  $\sigma_{n,p} \neq 0$  are present that allow much faster communication between the bands and Auger recombination will be negligible under low injection. Shockley-Read-Hall recombination is modeled by the definition of a proper recombination center (no lifetime parameter is present in the system). The system is solved numerically for pulse (illumination) and transient using an adaptive-step-size routine. The start occupations of all levels (in thermal equilibrium) are determined by calculating the Fermi level ( $E_F$ ) for a given level setup and temperature by computing the root of the charge neutrality condition. So the system starts at and relaxes back into thermal equilibrium for every given temperature. In contrast to low temperature studies of GaAs [11, 13] (e.g. simulations of the EL2 photoquenching effect), where equilibrium occupations of the bands are practically zero and can be neglected, they are important for the simulation of negative peaks for temperatures above 300 K, where transients are known to show a drop below equilibrium values [6].

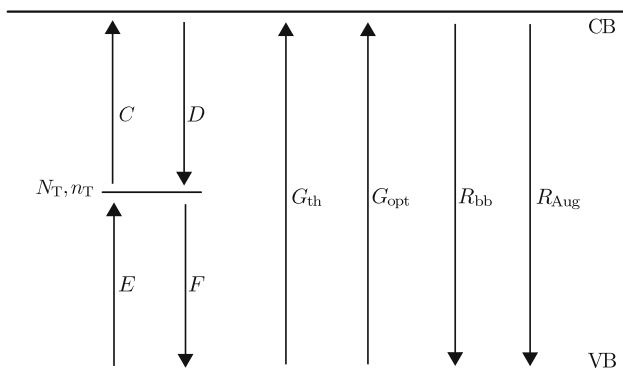


**Fig. 1** Semiconductor model with one artificial defect level and all considered band-band and defect-band interactions

### 3 The negative EL2 peak in SI-GaAs

MD-PICTS measurements on several carbon and zinc-doped SI-GaAs samples were performed using band-band excitation [14]. The resulting PICTS spectra (Fig. 2) show a clear Fermi level dependence of the negative peak effect. For  $E_F$  well above EL2, a negative peak can be observed while for lower  $E_F$ -values a positive peak is measured.

In order to investigate the conditions and system parameters under which a negative peak occurs, we set up a model according to Fig. 3. The expected relevant Fermi level regime for the occurrence of a negative peak lies sufficiently above the EL2<sup>+/+</sup> level ( $E_C + 0.54$  eV) [15, 16] so that it is filled and its contributions can be neglected. Additionally, a recombination center was used to account for the short lifetime ( $\approx 10^{-9}$  s) [5] in the material. Donor and acceptor levels are used to tune the  $E_F$  level (the Fermi level is not a parameter). As the measured quantity in PICTS is the sample conductivity, we

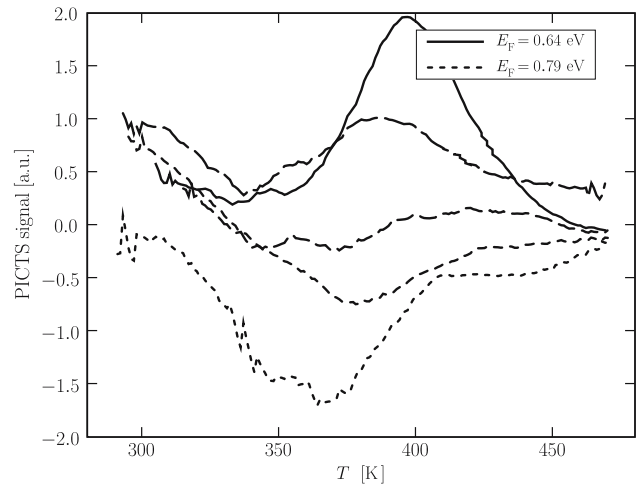


**Fig. 2** Measured positive and negative EL2 PICTS-peaks. Peaks from the experimental data [14] have been re-calculated for convenience (here using an initial delay  $t_1 = 30 \mu s$  in PICTS spectra generation)

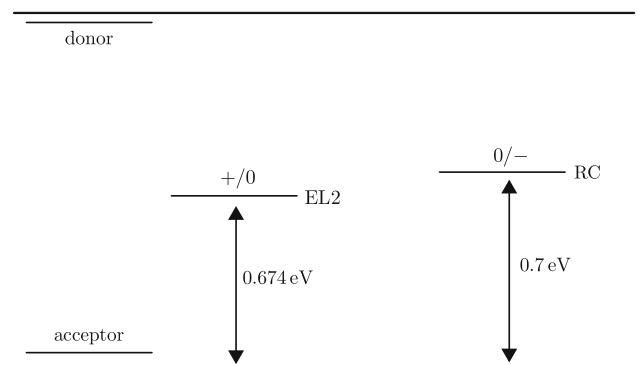


**Fig. 3** SI-GaAs model with EL2 and one recombination center (RC).  $N_{EL2} = 1.56 \times 10^{16} cm^{-3}$ ,  $N_{RC} = 1 \times 10^{14} cm^{-3}$

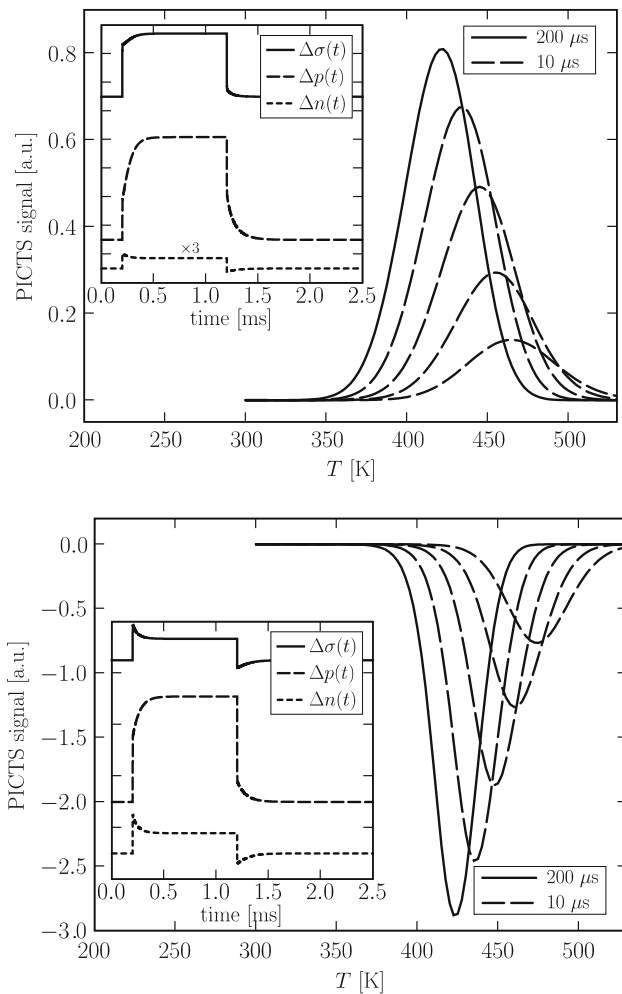


**Fig. 4** Example simulation results extracted from the performed calculations showing typical cases of a positive and negative peak for different  $t_1 = 10 \dots 200 \mu\text{s}$ . Upper panel:  $E_F = 0.76 \text{ eV}$ . Lower panel:  $E_F = 0.81 \text{ eV}$ . The peak swap occurs around  $E_F = 0.78 \text{ eV}$ . In both calculations:  $\sigma_{n,p}(\text{RC}) = 1.2 \times 10^{-15} \text{ cm}^2$ ,  $\sigma_p(\text{EL2}) = 2 \times 10^{-18} \text{ cm}^2$ ,  $\sigma_n(\text{EL2}) = 2.7 \times 10^{-16} \text{ cm}^2$ . The insets show the time dependence of  $\Delta n(t)$ ,  $\Delta p(t)$  and (scaled down)  $\Delta\sigma(t)$  around the peak maximum temperature. Note that in the upper panel,  $\Delta n(t)$  is scaled by a factor of 3 and that in both insets  $\Delta p(t)$  and  $\Delta\sigma(t)$  are shifted along the ordinate for convenience

calculated the PICTS signal from the simulated conductivity change  $\Delta\sigma = e_0(\mu_n\Delta n + \mu_p\Delta p)$  using a mobility ratio [17] of  $\mu_n/\mu_p = 20/1$ . As in the experimental investigation, a carrier generation (light pulse) time of 1 ms was used and PICTS data evaluation of the conductivity transients (signal after light cut-off) by a double-box-car technique [6, 18] with an initial time delay  $t_1 \geq 10 \mu\text{s}$  was applied.

#### 4 Simulation results

Example results from two simulation runs are shown in Fig. 4. In order to produce a negative peak, the

conductivity signal  $\Delta\sigma(t)$  has to have the form of that in the inset in the lower panel of Fig. 4, thus follow  $\Delta n(t)$  (or  $n(t) = n_0 + \Delta n(t)$ ). Such a  $n(t)$ -behavior can be explained as follows. During illumination, the EL2 acts as deep trap ( $\sigma_n \gg \sigma_p$ ) and captures free electrons from the CB. After light cut-off,  $n(t)$  shows a fast drop below the equilibrium concentration, which is caused by recombination through the RC, followed by a slow recovery originating in the thermal release of trapped electrons by the EL2. This mechanism can be verified by investigating the individual rates  $C$ ,  $D$ ,  $E$  and  $F$  at the EL2 and RC (not shown) and is supported by a parameter study explained below.

In a first simulation study, we varied the Fermi level from 0.65 eV ... 0.91 eV to check for a peak-swap from positive (low  $E_F$ ) to negative (high  $E_F$ ). Additionally, the cross sections of the RC have been changed simultaneously over a wide range from  $\sigma_{n,p}(\text{RC}) = 10^{-16} \dots 10^{-13} \text{ cm}^2$ . The EL2 cross sections [17, 19, 20] were set to  $\sigma_n = 2.7 \times 10^{-16} \text{ cm}^2$ ,  $\sigma_p = 2 \times 10^{-18} \text{ cm}^2$ . Also the optical generation rate was varied from  $10^{15} \dots 10^{20} \text{ cm}^{-3}\text{s}^{-1}$ . Since it was found that variations of the light intensity do only influence details of the pulse and transient forms but not the principal nature of the results, we restrict ourselves in the following to results from one parameter study, where the generation rate ( $8 \times 10^{17} \text{ cm}^{-3}\text{s}^{-1}$ ) assures the minimal injection to be  $\Delta\sigma/\sigma_0 > 1$  for all combinations of  $\sigma_{n,p}(\text{RC})$  and  $E_F$ .

Results are summarized in Fig. 5. It can be seen that for Fermi levels well above the EL2, a negative peak can be always found as long as  $\sigma_{n,p}(\text{RC}) \gg \sigma_n(\text{EL2})$ , i.e. recombination is faster than electron capture by the EL2 defect. In this study, negative peaks started to form for  $\sigma_{n,p}(\text{RC}) > 4 \times 10^{-16} \text{ cm}^2$  (for  $\sigma_n(\text{EL2}) = 2.7 \times 10^{-16} \text{ cm}^2$ ). The  $E_F$ -value for which a peak-swap from positive to negative occurs, depends on the RC cross sections and is situated above  $E_F = 0.7 \text{ eV}$ , which is in accordance with our measurements. For the minimal and maximal RC cross sections, for which a negative peak can be found, the peak-swap occurs at Fermi levels around 0.79 eV for  $\sigma_{n,p}(\text{RC}) = 4 \times 10^{-16} \text{ cm}^2$  and 0.73 eV for  $\sigma_{n,p}(\text{RC}) = 10^{-13} \text{ cm}^2$ .

Regarding lifetime, the calculations show that the desired small value of about  $\geq 10^{-9} \text{ s}$  can be achieved with  $\sigma_{n,p}(\text{RC}) \leq 10^{-13} \text{ cm}^2$ . Nevertheless, also for smaller cross sections (higher lifetime) a negative peak shows up, as long as recombination is fast enough, as mentioned above.

In order to investigate the relation between the RC cross sections (its recombination strength) and the electron capture cross section of the EL2 in a second study, we varied  $\sigma_n(\text{EL2})$  in the range  $10^{-13} \dots 10^{-16} \text{ cm}^2$  while setting  $E_F$  above the EL2 at 0.83 eV to ensure negative peak conditions and holding  $\sigma_{n,p}(\text{RC})$  constant at  $10^{-13} \text{ cm}^2$ . As  $\sigma_n(\text{EL2})$  decreases, the positive EL2-peak swaps to a negative one as soon as  $\sigma_n(\text{EL2})$  drops below  $10^{-14} \text{ cm}^2$ ,

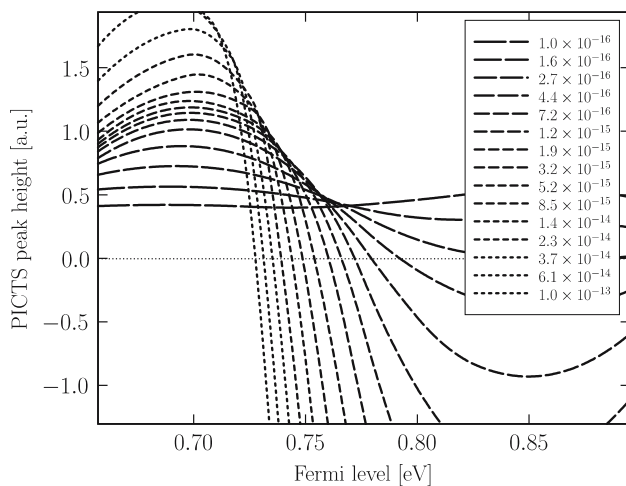


**Fig. 5** Dependence of the peak height (positive or negative) on the Fermi level and the RC cross sections  $\sigma_{n,p}$ (RC) (values in the legend in  $\text{cm}^2$ ). Peaks are calculated for  $t_1 = 30 \mu\text{s}$  from the same simulation data as in Fig. 4

i.e. the electron capture by the RC becomes faster than capture by the EL2.

### 5 Explanation of peak-swaps with a simplified rate equation model

The remaining question to be answered is the role of the Fermi level regarding the observed peak-swaps. A look at the calculated transients (insets Fig. 4) reveals that for both the positive and negative peak, the  $\Delta n(t)$ -transient shows “negative peak behavior” while the  $\Delta p(t)$ -transient would give rise to a positive peak. As mentioned above, the signal processed with PICTS data evaluation is the conductivity change  $\Delta\sigma = e_0(\mu_n \Delta n + \mu_p \Delta p)$ . As can be seen in Fig. 4, the  $E_F$ -value influences the relative magnitudes of  $\Delta n$  and  $\Delta p$ , thus giving rise to positive and negative peaks. A qualitative explanation can be derived from a simplified trap model [21]. The model compares a trap-free semiconductor to a semiconductor containing a pure electron trap.

- (i) Carrier dynamics in a trap-free semiconductor, having its lifetime  $\tau$  ( $\equiv \tau_n \equiv \tau_p$ ) determined by a SRH center, can be described by the simplified rate equations  $\dot{n} = -n/\tau + G_{\text{opt}}$  and  $\dot{p} = -p/\tau + G_{\text{opt}}$ . In steady state under illumination ( $\dot{n} = \dot{p} = 0$ ) the concentration of excess carriers is  $\Delta n_1 = \Delta p_1 = \tau G_{\text{opt}}$ .
- (ii) If a non-zero concentration of electron traps is present, the rate equations read  $\dot{n} = -n/\tau + G_{\text{opt}} + C - D$ ,  $\dot{n}_T = -C + D$  and  $\dot{p} = -p/\tau + G_{\text{opt}}$ , again assuming the lifetime  $\tau$  for  $n$  and  $p$ . In steady state  $C - D = \dot{n}_T = 0$  and the excess electron concentration is again  $\Delta n_2 = \tau G_{\text{opt}} = \Delta n_1$ . Now, additional  $\Delta n_T$  electrons are trapped and the conservation of charge requires  $\Delta n_1 + \Delta n_T = \Delta p_2 > \Delta p_1$ .

The amount of trapped electrons and thus the ratio  $\mu_n \Delta n / \mu_p \Delta p$  is determined by the initial occupation of the trap and therefore by the Fermi level. For “high” Fermi levels, less electrons can be captured as the trap is already well occupied. Even though  $\Delta p > \Delta n$  because of the presence of the trap, the mobility difference assures that  $\mu_n \Delta n > \mu_p \Delta p$  which results in a negative peak. For lower Fermi levels the trap is less filled and captures more free electrons. This leads to  $\Delta p \gg \Delta n$  and so  $\mu_n \Delta n < \mu_p \Delta p$  thus giving rise to a positive peak.

### 6 Conclusion

The above investigations have reproduced the measured  $E_F$ -dependence of the PICTS peak-swap from positive to negative sign and support the proposed model for the formation of a negative EL2 peak. The negative peak could be observed over a rather broad range of cross section values for EL2 and RC, while the relevant Fermi level regime for a peak-swap is relatively constant between  $\approx 0.7 \dots 0.8$  eV. The only requirements for the negative EL2 peak can therefore be formulated as (i) a deep trap state (the EL2 with  $\sigma_p \ll \sigma_n$ ) and (ii) a fast recombination channel (faster than the electron capture by the trap). (iii) The appearance of a negative peak depends on the Fermi level before illumination. The third condition has been explained by a simple trap model.

The assumption of a fast RC, as is used here, has been widely discussed. Some authors have argued that the EL2 itself should be viewed as the recombination center [22]. As this may very well be the case (since  $\sigma_n, \sigma_p \neq 0$ ), the observed effect of negative peaks and its relation to the Fermi level could not be reproduced with only one center, either RC or EL2 alone, in all our calculations.

**Acknowledgment** We wish to thank Freiburger Compound Materials GmbH for kindly providing the investigated samples.

### References

1. B. Gründig-Wendrock, M. Jurisch, J.R. Niklas, *Mat. Sci. Eng.* **B91–92**, 371 (2002)
2. T. Steinegger, B. Gründig-Wendrock, M. Jurisch, J.R. Niklas, W. Jantz, M. Baeumler, *Mat. Sci. Eng.* **B91–92**, 29 (2002)
3. B. Gründig-Wendrock, J.R. Niklas, *Phys. Stat. Sol.* **0**, 885 (2003)
4. M. Ogawa, T. Kamiya, H. Yanai, *Inst. Phys. Conf. Ser.* **63**, 571 (1982)
5. M.J.S.P. Brasil, P. Motisuke, *J. Appl. Phys.* **68**, 3370 (1990)
6. S.R. Blight, H. Thomas, *J. Appl. Phys.* **65**, 215 (1988)
7. R.E. Kremer, M.C. Arikian, J.C. Abele, J.S. Blakemore, *J. Appl. Phys.* **62**, 2424 (1987)
8. V.C. Lo, P.W. Chan, S.D. Xu, S.P. Wong, *Semicond. Sci. Technol.* **7**, 668 (1992)
9. M. Müllenborn, H.C. Alt, A. Herbele, *J. Appl. Phys.* **69**, 4310 (1991)

10. O. Yoshie, M. Kamihara, *Jpn. J. Appl. Phys.* **22**, 621 (1983)
11. M. Pavlović, B. Šantić, D.I. Desnica-Franković, N. Radić, T. Šmuc, U.V. Desnica, *J. Electron. Mater.* **32**, 1100 (2003)
12. K.W. Böer, *Survey of Semiconductor Physics, Second Edition, Electrons and Other Particles in Semiconductors*, vol 1 (Wiley, 2002)
13. A.A.J. Jiménez, M.A. González, L.F. Sanz, *Appl. Phys. Lett.* **70**, 3131 (1997)
14. B. Gründig-Wendrock, K. Dornich, T. Hahn, U. Kretzer, J.R. Niklas, *Eur. Phys. J. Appl. Phys.* **27**, 363 (2004)
15. A. Fukuyama, A. Memon, K. Sakai, T. Ikari, *J. Appl. Phys.* **89**, 1751 (2001)
16. P. Omling, P. Silverberg, L. Samuelson, *Phys. Rev. B* **38**, 3606 (1988)
17. D.C. Look, Z.-Q. Fang, *J. Appl. Phys.* **80**, 3590 (1996)
18. P. Blood, J.W. Orton, *The Electrical Characterization of Semiconductors: Majority Carriers and Electron States* (Academic Press, London, 1992)
19. G.M. Martin, S. Makram-Ebeid, The Mid-Gap Donor Level EL2 in GaAs, in *Deep Centers in Semiconductors*, 2nd edn., ed. by S.T. Pantelides (Gordon and Breach Science Publishers, 1992), pp. 457–545
20. D.C. Look, Z.-Q. Fang, J.R. Sizelove, *J. Electron. Mater.* **24**, 1461 (1995)
21. J.A. Hornbeck, J.R. Haynes, *Phys. Rev.* **97**, 311 (1955)
22. J.C. Bourgoin, N.D. Angelis, *Semicond. Sci. Technol.* **16**, 497 (2001)